ChemComm

Photosynthetic biohybrid systems for solar fuels catalysis

Journal:	*ChemComm*
Manuscript ID	CC-FEA-02-2024-000774.R3
Article Type:	Feature Article

ARTICLE

Photosynthetic biohybrid systems for solar fuels catalysis

Lisa M. Utschig* and Karen L. Mulfort

Received 00th January 20xx,
Accepted 00th January 20xx

DOI: 10.1039/x0xx00000x

Photosynthetic reaction center (RC) proteins are finely tuned molecular systems optimized for solar energy conversion. RCs effectively capture and convert sunlight with near unity quantum efficiency utilizing light-induced directional electron transfer through a series of molecular cofactors embedded within the protein core to generate a long-lived charge separated state with a useable electrochemical potential. Of current interest are new strategies that couple RC chemistry to the direct synthesis of energy-rich compounds. This Feature Article highlights recent work from our lab on RC and RC-inspired hybrid systems that capture the Sun's energy and convert it to chemical energy in the form of H_2, a carbon-neutral energy source derived from water. Biohybrids made from the Photosystem I (PSI) RC are among the best photocatalytic H_2-producing protein hybrids to date. Targeted self-assembly strategies that couple abiotic catalysts to PSI translate to catalyst incorporation at intrinsic PSI sites within thylakoid membranes to achieve complete solar water-splitting systems. RC-inspired biohybrids interface synthetic photosensitizers and molecular catalysts with small proteins to create photocatalytic systems and enable the spectroscopic discernment of the structural features and electron transfer processes that underpin solar-driven proton reduction. In total, these studies showcase the incredible scientific opportunities photosynthetic biohybrid research provides for harnessing the optimal qualities of both artificial and natural photosynthetic systems and developing materials that capture, convert, and store solar energy as a fuel.

Introduction

Photosynthetic organisms utilize solar radiation to convert light into chemical energy, ultimately synthesizing energy-rich compounds from abundant but thermodynamically stable inputs like water and CO_2. The primary photosynthetic energy conversion reactions occur in large integral membrane protein complexes called reaction centers (RCs).[1] Three of the best-known RCs are the bacterial RC from purple non-sulfur bacteria and the Photosystem I (PSI) and Photosystem II (PSII) RCs found in higher plants, algae and cyanobacteria. All RCs consist of a dimeric core with two nearly symmetrical potential electron donor/acceptor chains that extend across the membrane (Fig. 1). Light-harvesting antenna complexes funnel excitation energy to this RC core and initiate a series of rapid, sequential electron transfers through the molecular cofactor chain(s) that results in formation of a stabilized charge separated state whose lifetime is in the millisecond range dependent on RC type. This incredibly long-lived charge separated state occurs with near unity quantum efficiency. Nature supports this process by the evolutionary-tuned protein-cofactor interactions where the large protein structures act as scaffolds to precisely position each molecular cofactor at the optimal distances and geometries with respect to each other, enabling efficient electron transfer. The local anisotropic environment hosting these redox sites dynamically adjusts to promote and steer directional electron transfer, stabilize the charge separated state, and provides mechanisms to couple with secondary reaction sequences.

Building on what has been learned from RCs and photosynthetic organisms, artificial photosynthetic systems aim to structurally or functionally mimic parts of nature's intricate molecular machinery using known chemical principles, and synthetic chemistry and materials science approaches. For decades, the RC cascade of

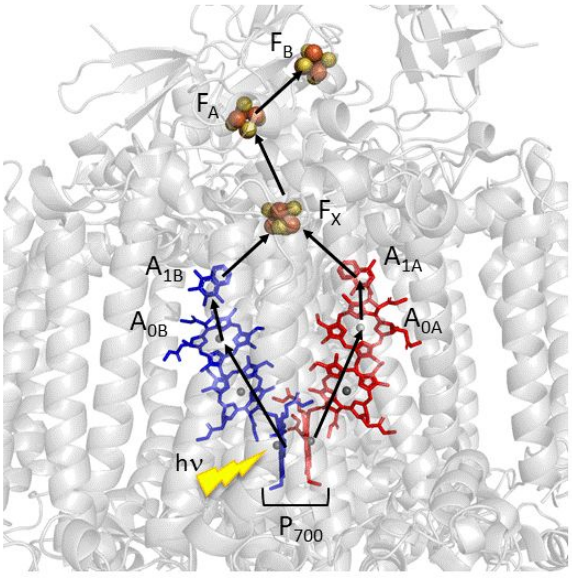

Fig. 1 Subset of the crystal structure of Photosystem I (PSI) Reaction Center (PDB: 1JB0) highlighting the core cofactors and electron transfer pathways that support the formation of the charge-separated state $P700^+F_B^-$ by rapid, sequential electron transfers between the cofactors initiated by solar excitation.

Chemical Sciences and Engineering Division, Argonne National Laboratory, Lemont, IL 60439, USA. E-mail: utschig@anl.gov

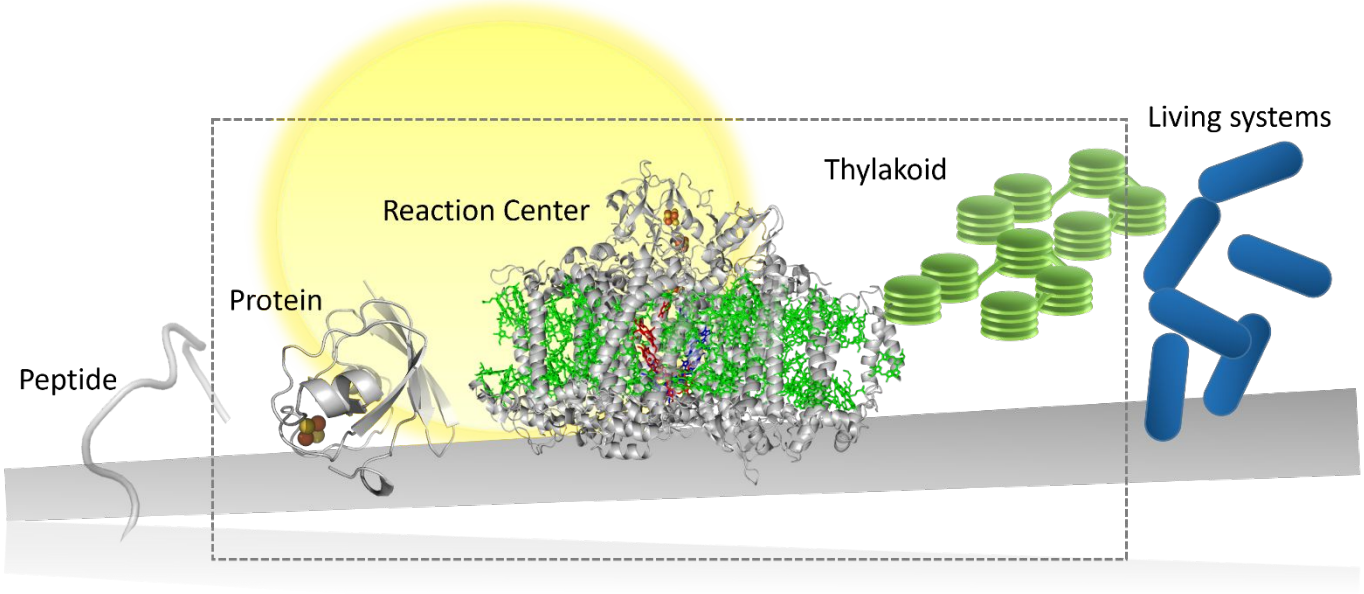

Figure 2. Biological scaffolds used in photosynthetic biohybrid designs range in size and complexity from minimalist peptides to bacteria. The biohybrid architectures discussed here are included in the dashed rectangle and are composed of small electron shuttle proteins, the Photosystem I RC, and thylakoid membranes.

electron donor/acceptor cofactors has inspired synthetic designs for multistep electron transfer constructed of self-assembled and covalently bound donor and acceptor molecules.[2-4] This foundational work has led to efforts focused on connecting molecular photosensitizers and electron transfer relays to synthetic molecular catalysts to yield photocatalyst architectures that use solar energy to transform abundant chemicals into fuels and other useful chemicals (i.e. hydrogen from water and hydrocarbons from CO_2).[5, 6] Molecular, multi-molecular, supramolecular and hybrid nanoparticle-molecule systems provide a wide range of synthetic approaches[7-9] to address the challenges of efficient coupling of single-photon/electron events with multielectron redox reactions necessary for fuel generation by building in functional sites for light-harvesting, charge transport, substrate capture, charge accumulation, and redox reactions.[10] A comprehensive evaluation of the total efficiency of natural photosynthesis shows that, since artificial photosynthetic systems aren't required to divert captured solar energy to support reproduction and growth like photosynthetic organisms do, they can be synthetically tuned for specific chemical reactions, potentially surpassing the direct photons-to-fuels efficiency of natural photosynthesis.[11, 12]

Despite the enormous potential for artificial photosynthetic systems, purely synthetic or abiotic architectures cannot replicate the structural complexity and hierarchy that create localized heterogeneous and dynamic protein environments that are critical for managing photons-to-fuels catalysis. Photosynthetic "biohybrid" architectures, however, combine the evolved protein architectures from biology with the structural creativity and specialized chemical properties provided by synthetic materials. The first description of a synthetically-modified RC was reported by Greenbaum and co-workers and involved photochemical deposition of metallic Pt on chloroplast thylakoids resulting in photocatalytic H_2 and O_2 evolution.[13] Since that seminal work, biohybrid research has expanded dramatically to encompass a wide range of proteins, natural architectures, and augmentation by numerous abiotic cofactors. RC biohybrids direct the protein's optimized photochemistry to localize the charge-separated state on abiotic catalysts inserted into the protein framework.[14] For many of these architectures, the use of H_2 evolution catalysts and demonstration of light-induced H_2 production confirms that the abiotic catalyst is indeed coordinated with the protein framework and on the acceptor end of the RC charge separation pathway.[15-17]

Much of the early biohybrid work focused on integrating Pt nanoparticles or other precious metal nanoparticles that are known to promote H_2 evolution into RCs, but molecular catalysts provide a greater degree of synthetic control over the active site. Further, because of their relative abundance on earth, first-row transition-metal based molecular catalysts provide a scalable alternative to benchmark hydrogen evolution catalysts such as platinum and hydrogenases.[18, 19] Along these lines, molecular catalysts based on cobalt, nickel, and iron have been modified to specifically interact with various protein architectures and the resulting biohybrids are photocatalytically active for H_2 evolution and CO_2 reduction.[20-30] In several cases, H_2 evolution activity is observed from biohybrid architectures composed of molecular catalysts who show minimal activity under similar conditions, indicating an important synergistic role of the protein environment to enable activity under biologically-relevant, mild conditions.[31-33] Also, interfacing molecular catalysts with proteins provides opportunity to add specific functionality or spectroscopic handles to gain otherwise unattainable insight about enhanced light-driven chemical reactions.[31-34] Importantly, well-designed biohybrid architectures enable the spectroscopic

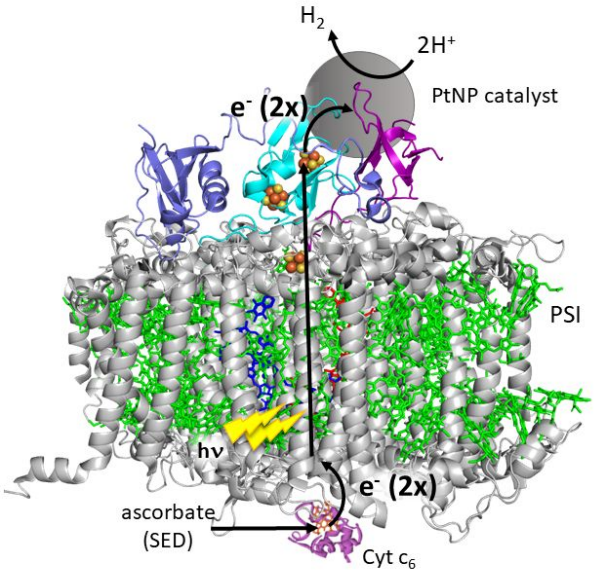

Fig. 3 Scheme of photocatalytic H_2 production by a PSI-PtNP biohybrid. The electrostatically-associated PtNP at the stromal side allows the accumulation of two successive photogenerated electrons from PSI required for H_2 generation from water. (PDB: 1JB0)

delineation of dynamic light-induced electron transfer processes crucial to solar-driven proton reduction.[29, 31-33]

Another important class of biohybrids links photo- and redox-active synthetic materials to enzymes. The light-harvesting synthetic components typically undergo an internal photoinduced charge transfer or charge separation event which then enables electron transfer across the biohybrid interface to drive native enzymatic reactions using light energy input.[18, 35, 36] Specific examples include various nanomaterials that have been successfully linked to hydrogenases, dehydrogenases, and nitrogenase for solar fuel reactions, creating H_2, formate and CO from CO_2, ammonia from N_2.[37-43] This work has been extended to living systems in which nanomaterials are interfaced with microorganisms.[44-46]

In this Feature Article, we highlight our team's work on RC and RC-inspired biohybrids as approaches to investigate and utilize solar energy in photons-to-fuels schemes that functionally mimic photosynthesis. The biohybrid field of study is rich, spanning multiple levels of biological hierarchy (Fig. 2). Minimalist peptide chains whose secondary structure can accommodate insertion of a transition metal complex or cation have been designed to include proton transfer relays and are photo- and electro-catalytically active for aqueous H_2 evolution.[47-50] Other efforts incorporate catalysts into full protein structures and require diffusional interaction with photosensitizer molecules in solution for photocatalysis.[20-30] Moving up in complexity, our group and others have used relatively small electron transfer proteins with or without their native cofactors to position both molecular photosensitizers and catalysts in protein scaffolds, creating a mini-RC biohybrid.[31-33, 51] Positioning abiotic catalysts near the terminal acceptor (F_B) site of the PSI RC exploits the strong light-absorption and highly efficient charge separation to divert the photogenerated electrons to the catalysts, enabling charge accumulation leading to catalytic activity.[15-17, 34, 52-55] This work has been extended to catalyst incorporation with thylakoid membranes to split water into H_2 and O_2.[56] Within this broad scope, we have focused on using RC and closely related proteins as the foundation for our biohybrids. This work stems from our deep knowledge of PSI structure and expertise in selectively removing native cofactors that have enabled detailed spectroscopic studies to obtain a high-resolution map of photoinduced charge separation.[57-61] Here we will describe several examples of biohybrid architectures from our work and discuss the results in the context of artificial photosynthesis in general.

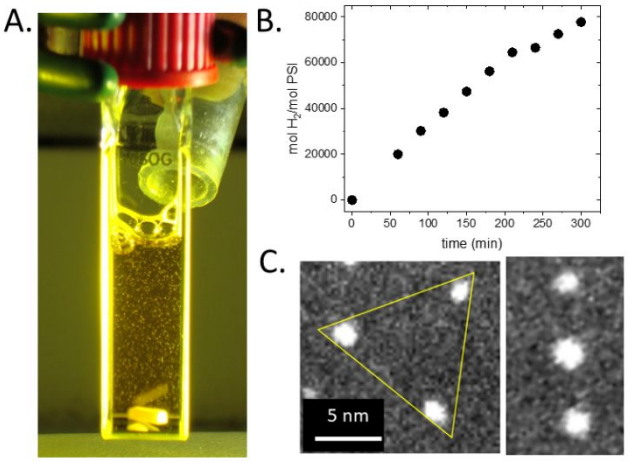

Fig. 4 A. Photograph of the experimental reaction during illumination showing H_2 bubbles of an anaerobic solution of a 100 nM PSI-PtNP hybrid with 100 mM sodium ascorbate and 4 μM cytochrome c_6.[17] B. Time course of H_2 production of a PSI-PtNP hybrid upon illumination with visible light. C. High angle annular dark field (HAADF) scanning transmission electron microscopy (STEM) images of thylakoid-PtNP hybrids showing the trimeric formation in planar (left) and linear arrangement (right).[78]

Photosystem I-Pt nanoparticle biohybrid

The PSI RC is a large, integral membrane protein complex composed of 12 protein subunits and 127 cofactors.[62] In oxygenic photosynthesis, PSI initiates and sustains light-driven electron transfer across the thylakoid membrane between plastocyanin in the lumen to ferredoxin (Fd) in the stroma. Sequential electron transfer occurs after the primary electron donor P700 (a dimer of chlorophyll molecules) becomes oxidized following photoexcitation, with concurrent electron transfer to A_0, a chlorophyll molecule, and A_1, a phylloquinone (Fig. 1). From A_1^-, the electron is transferred to F_X, an [4Fe-4S] cluster, and then further to two additional [4Fe-4S] clusters F_A and F_B which are positioned within the extrinsic protein subunit PsaC. F_B^- then transfers the photogenerated electron to the small soluble acceptor protein Fd, or flavodoxin (Fld) in conditions of low iron, which then shuttles the reducing equivalents from PSI to several metabolic pathways. PSI has a quantum yield that approaches 1 – hence nearly all photons absorbed are converted to the charge-separated state $P700^+F_B^-$. This charge-separated state has a lifetime of 60 ms and a favorable electrochemical potential of -580 mV for the terminal F_B cluster, and therefore PSI is the ideal RC to photochemically drive H_2 production (E_m, pH 6.3 = -370 mV).[63] PSI's photogenerated electrons have been successfully coupled to

hydrogenase enzymes[19, 52, 63-65] and platinum catalyst systems.[15-17, 53, 54, 66-68] Following the first report of platinized chloroplasts,[13] photodeposition of metallic Pt onto isolated PSI has been continued to be studied.[54, 68-71]

In 2008, Grimme et al. reported a biohybrid in which a Pt-nanoparticle (PtNP) was directly tethered via a dithio molecular wire to a mutated [4Fe-4S] F_B cluster of a subunit-stripped PSI.[16] This biohybrid achieved rates of H_2 production several orders of magnitude higher than prior photoprecipitated Pt-based systems. The increased rates were attributed to the 1,6-hexanedithiol linker

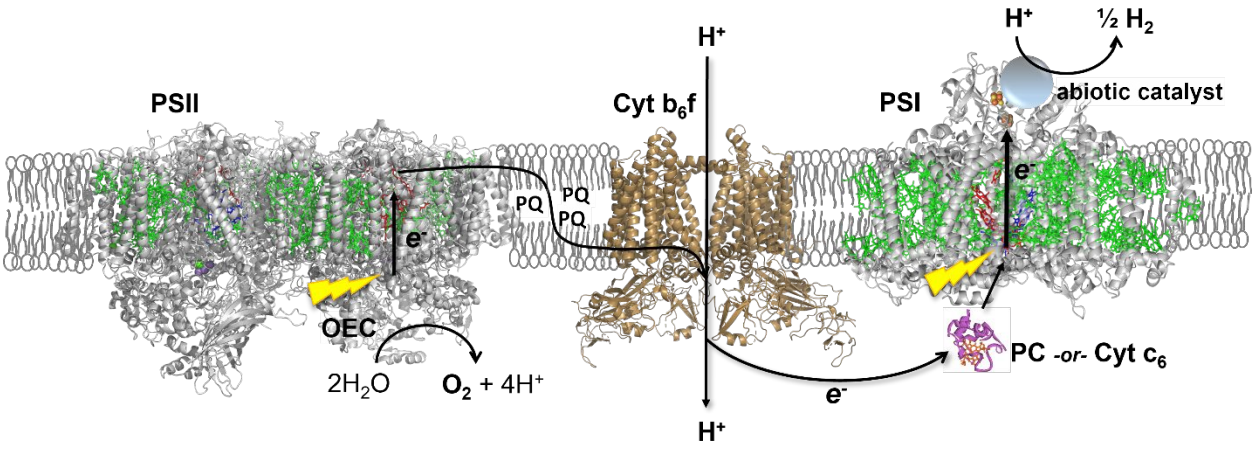

Figure 5. Schematic representation of the abiotic PtNP self-assembled with the stromal end of PSI for Z-scheme electron transport driven splitting of water into O_2 and H_2. Photosystem II (PSII) absorbs visible photons to initiate water oxidation by the oxygen-evolving complex (OEC). The electrons ejected from the water oxidation process are transferred to PSI via the plastoquinone (PQ) pool, the cytochrome b_6f complex (Cyt b_6f), and one of the luminal electron transfer proteins plastocyanin (PC) or cytochrome c_6 (Cyt c_6). Following light excitation, PSI transfers photogenerated electrons from the lumen to the stroma of the thylakoid membrane where the soluble electron transfer proteins Fd or Fld are reduced. In our membrane-bound biohybrid system, abiotic catalysts positioned at the Fd/Fld acceptor end of PSI utilize the light-generated electrons to catalyse H_2 generation from water. Protein structures: PSII (2axt), Cyt b_6f (2D2C), cyt c_6 (1c6s), PSI (1JB0)

molecule directing electrons from F_B the PtNP.[63, 67] This work inspired us to leverage PSI-PtNP complexation, except in our case, extending the concept to native PSI with no mutations. The strategy we developed to incorporate abiotic catalysts at the acceptor end of PSI was to mimic acceptor protein binding (Fig. 3). Three protein subunits, PsaC, PsaD, and PsaE, form the stromal hump of PSI and are involved in the docking of Fd. The interaction between PSI and Fd is electrostatically-driven with the negatively charged surface of Fd docking to a positively charged region found on PSI.[72, 73] To synthesize the PSI-PtNP biohybrids, we first prepared 3 nm PtNPs according to literature methods[74] and then added 1.2- 2.0 mol equivalents of the PtNP colloidal aqueous solution to PSI protein that was isolated from the cyanobacteria *Synechococcus leopoliensis* or *Synechococcus lividus.* The standard procedure for isolation of PSI [75, 76] includes isolation of the thylakoid membranes from a suspension of cyanobacteria by disrupted with a Bead Beater (BioSpec Products, Inc) with 0.1 mm glass beads. The PSI protein is solubilized from the membranes by addition of 1% n-dodecyl-β-D-maltopyranoside (Anatrace) 0.1 % Triton followed by separation on a sucrose density gradient. It is well-established by over 50 years of EPR and optical studies that PSI retains its light harvesting and charge separation capabilities when isolated from the thylakoid membrane.[1] The PSI-PtNP biohybrid was isolated from excess unbound PtNPs by microfiltration with Amicon 50000 MWCO filtration devices. PSI-PtNP biohybrids were washed multiple times by repeated resuspension/concentration steps. ICP-AES (inductively coupled plasma atomic emission spectroscopy) confirmed a 1 PSI: 1 PtNP ratio by comparing the Fe and Pt content in from the native 4Fe-4S cluster in PSI and 940 Pt atoms calculated to be present in 3 nm NPs.[17] Thus, in our system, we demonstrated that mercaptosuccinic acid stabilized PtNPs, with a similar size and charge as Fd, stoichiometrically bind to PSI.[17] EPR spectroscopy confirmed that the PtNP functionally mimics acceptor protein binding to PSI, as we clearly observed the same altered charge-separation when PtNP or flavodoxin (Fld) are bound to PSI.[17, 77] Furthermore, when PtNP is associated with PSI electron transfer to excess Fld in solution is inhibited.[17] Based on these observations, we hypothesized that the PtNP assembles with PSI similar to the native ET protein Fld. This self-assembled, noncovalent, electrostatically-associated PSI-PtNP biohybrid is a highly active photocatalyst, achieving over 21,000 turnovers of H_2 per hour, the highest rate achieved to date for a PSI platinum system (Fig. 4A, B).[17] Not only is catalyst positioning on PSI important to achieve rapid photocatalysis, but also important are the donor side reactions. As PSI transfers one electron at a time to the catalyst site, oxidized $P700^+$ needs to get rapidly reduced so that two successive electrons arrive at the bound catalyst site for generation of one hydrogen molecule. Therefore, the photocatalytic reaction conditions for isolated PSI biohybrid systems include the sacrificial electron donor (SED) sodium ascorbate and the native donor protein to PSI, cytochrome c_6. This study provides a proof of concept for the reductive photochemistry for self-assembled PSI-based biohybrids, and inclusion in thylakoid membranes provide a means to remove the need for SED and extend studies from proton reduction to the complete water-splitting reaction.

Thylakoid-Pt nanoparticle hybrids

In oxygenic photosynthesis, PSII and PSI work together in a coupled electron transfer Z-scheme: light-driven oxidation of water is performed by the OEC of PSII whereas PSI promotes light-driven transmembrane electron transfer to an external acceptor protein.[1]

These electrons are then used to produce NADPH, an electron source for Calvin cycle CO_2 fixation. This native Z-scheme electron transport chain can be utilized to generate hydrogen by hijacking the electrons meant for NADPH formation by direct electron transport to abiotic catalysts bound to the stromal end of PSI, negating the need for a SED (Fig. 5). The self-assembling strategy of electrostatically charged PtNP is translatable to the *in situ* thylakoid environment as the stromal end of PSI extends beyond the membrane plane and is solvent accessible for assembly with abiotic catalyst. To synthesize the thylakoid-PtNP hybrids, fresh thylakoids were prepared from spinach, *S. leopoliensis*, and *S. lividus*. [56] The viability of the thylakoids was verified by measuring the oxygen evolution activity with a Unisense Oxy-NP probe. Thylakoids, at a concentration of 0.7 mg ml^{-1} chlorophyll (Chl) were incubated with 1.2 μM of 3 nm mercaptosuccinic acid PtNPs that were synthesized by literature procedures[74] overnight. The thylakoid membranes were pelleted, the supernatant removed, followed by careful resuspension in pH 6.0 buffer. The samples were then repelleted and this was repeated 3 times to remove any unassociated PtNP from the membrane surface. The resultant thylakoid-PtNP hybrids were resuspended in solution and illuminated. We observed light-driven H_2 production in the presence of a SED and the mediating electron shuttle protein cytochrome c_6, suggesting that the PtNPs readily self-assemble with both spinach and cyanobacterial thylakoids (*Synechococcus leopoliensis*) (Table 1).[56] We also monitored the light-driven H_2 production in the absence of a SED, leaving PSII as the only source of electrons to regenerate $P700^+$, and found that H_2 production at PSI occurs via coupling to light-induced PSII oxygen evolution – thus achieving complete solar water splitting![56] Similar to the PSI-PtNP work, EPR spectroscopic characterization of photoinduced electron transfer was consistent with placement of PtNP at the acceptor end of PSI.[56] We were able to conclusively confirm the location of the PtNPs using STEM imaging of the thylakoid-PtNP biohybrids, providing the first direct visualization of the water-splitting system (Fig. 4C).[78] STEM hyperspectral elemental imaging of Pt, Mg, S, and Fe confirmed co-location of Pt sites at intrinsic PSI membrane sites. Trimeric configurations of PtNPs in cyanobacterial thylakoids mimic the trimeric configuration of Fld and Fd observed in cryoEM and crystal structures of trimeric PSI-Fld and PSI-Fd complexes. [72, 79-81]

Interestingly, the majority of PtNPs appeared to be associated to only one monomer of the PSI trimer. More recent work from our group provides evidence of *in situ* Fd association with thylakoid membranes which could prevent catalyst binding.[82] Thus, an important opportunity to increase overall photocatalytic activity of the thylakoid-PtNP systems is to determine methods to bind abiotic catalysts to each monomer of the PSI trimer in cyanobacterial thylakoid environments.

Photosystem I-molecular catalyst biohybrids

The PSI-PtNP biohybrids—whether using isolated or membrane-bound PSI—provided an important foundation for our understanding of how abiotic cofactors can utilize similar self-assembly mechanisms that are hallmarks of protein-protein interactions prevalent in biology.[17, 56, 78] However, we were motivated to replace the PtNPs with molecular H_2 evolution catalysts for two key reasons. First, a sizeable majority of molecular H_2 catalysts described in the literature are transition metal coordination complexes,[83-88] and the synthetic versatility of this class of molecules provides chemists the ability to tune a catalyst's molecular and electronic structure with high spatial resolution. The electrochemical potential of a catalyst in its ground-, oxidized-, or reduced-state directly influences a catalyst's ability to accept photogenerated electrons from PSI and use them for H—H bond formation. Fine-tuning the optical properties of an abiotic catalyst may introduce useful spectral features that can be used to track electron transfer kinetics, catalyst oxidation state, or coordination environment. The synthetic versatility also introduces the possibility to append a molecular catalyst with handles that can covalently bind to specific protein residues in case electrostatic interactions or other self-assembly mechanisms are not possible or efficient. Second, embedding molecular catalysts with protein scaffolds introduces unique opportunities for molecular activity in this new microenvironment. For example, protein folds and specific residues can provide locations for proton transfer or docking, critical components to help manage disparate timescales of proton and electron transfer. Also, the native electron transfer relay of PSI has provided much of the inspiration for elaborate molecular donor-acceptor systems,[2, 4] but in a biohybrid we can use the exact evolutionarily-optimized cofactors to shuttle electrons to the catalyst active site. Importantly, the dynamic and heterogeneous environment found within a protein's secondary or tertiary structure is incredibly challenging, if not impossible, to replicate synthetically but enables important mechanisms for stabilizing charge accumulated states and preventing unproductive charge recombination. And finally, many molecular H_2 evolution catalysts are not soluble or active in aqueous solution, the ideal solvent for water-splitting catalysis. However, our work has shown that biohybrids consisting of molecular catalysts can be very active and long-lived in biologically-relevant conditions, suggesting that the protein environment provides important stabilization for the molecular complexes throughout the catalytic cycle.

Cobaloximes were the first type of molecular catalyst we targeted for PSI incorporation. We chose these pseudomacrocyclic bis(dimethylglyoxamato) cobalt catalysts because of their demonstrated ability to reduce protons either electro- or photocatalytically, relative ease of synthesis, tolerance of O_2 in their ground state, well-documented mechanism for proton reduction, and use of only earth-abundant elements.[7, 89-94] The rapid photocatalysis that we observed for the self-assembled PSI-PtNP biohybrid demonstrated that covalent linkage between catalyst and PSI was not necessary for light-driven aqueous H_2 evolution. Therefore, a similar self-assembly strategy was developed for a PSI biohybrid that incorporates a molecular catalyst rather than PtNPs.[55] Dark-adapted PSI (isolated from *S. leopoliensis* or *S. lividus*) in a 20 mM Hepes (pH 6.9) buffered solution was incubated with excess of the cobaloxime derivative $Co(dmgH)_2pyCl$ (where dmgH = dimethylglyoximate, py = pyridine) (Fig. 6A, CoPy) that was synthesized from published procedures.[93] Typically 2-10 mol equivalents of CoPy from a stock solution prepared in DMSO was added to a 5 μM solution of PSI, incubated for 2 hours in the dark. Unbound catalyst was removed by size exclusion methodologies. ICP-AES was used to determine the number of Co catalysts bound per PSI monomer. Upon exposure to visible light, the resultant PSI-cobaloxime biohybrid rapidly produced H_2 from aqueous buffered solution at pH 6.3 with sodium ascorbate as the SED and excess cyt c_6 to re-reduce $P700^+$ (Fig. 6C).

Following the methodology developed for cobaloxime, a second PSI-molecular catalyst hybrid was constructed using a Ni(II)bis(diphosphine) catalyst developed by DuBois and coworkers

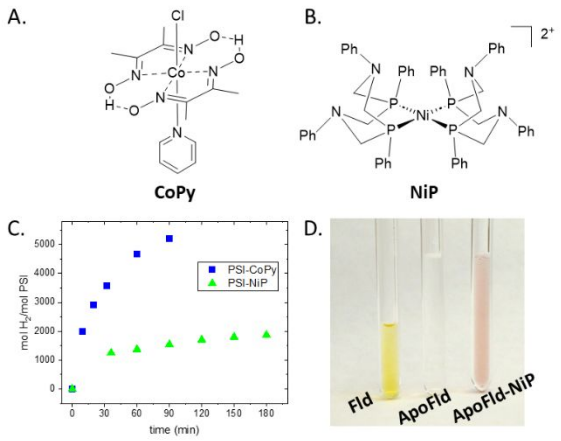

Fig. 6 A. $Co(dmgH)_2pyCl$ (where dmgH = dimethylglyoximate, py = pyridine), B. $[Ni(P_2^{Ph}N_2^{Ph})_2](BF_4)_2$, C. Time course profile of H_2 production upon illumination of PSI-CoPy and PSI-NiP hybrids.[34, 55] D. Protein solutions of native Fld, ApoFld, and ApoFld-NiP hybrid.[32]

(Fig. 7A).[34] These DuBois-type catalysts have the general formula $[Ni(P_2^RN_2^{R'})_2]^{2+}$ (where $P_2^RN_2^{R'}$ is 1,5-R'-3,7-R-1,5-diaza-3,7-diphosphacyclooctane and R and R' are substituents on the phosphine and amine units, respectively), and are some of the most active 3d transition-metal electrocatalysts for proton reduction, with pendant amines in the secondary coordination sphere that function as proton relays to accelerate H-H bond formation.[95-97] We found that $[Ni(P_2^{Ph}N_2^{Ph})_2](BF_4)_2$ (Fig. 6B, NiP) assembled with PSI in buffered solution at pH 7.3 in ratios dependent on the initial amount of Ni catalyst bound to the protein, similar to CoPy complex formation with PSI.[34] Self-assembly resulted in an active biohybrid that produces H_2 at rates two orders of magnitude greater than rates for a comparable artificial multi-molecular photosensitizer and NiP system.[98] Notably, the protein environment enabled photocatalysis in completely aqueous conditions at pH 6.3 – much milder conditions than the strong acid requirement (pH 2) for rapid electrocatalytic and artificial photocatalytic hydrogen production reported for NiP alone in solution.[98, 99] Our hypothesis to explain this observation is that biohybrid formation is dominated by hydrophobic interactions, with the molecular catalysts simply tucking themselves into hydrophobic pockets provided by large PSI protein complex (350 kDa per monomer).[34] Importantly, the photocatalytic activity of these biohybrids is key evidence supporting the effective accumulation of the rapidly formed, single electron photo-excited charge separated states of PSI at the transition metal catalyst sites which manage the slower multiple proton-coupled ET required for H_2 generation from aqueous protons (Table 1). A notable drawback of the PSI-molecular catalyst systems, however, is the short lifetime of the observed photocatalysis. We measured very fast initial rates immediately upon light exposure for 10-30 min, which then leveled off at < 1.5 hours for CoPy and < 3 hours for NiP (Fig. 6C).[34, 55] After photocatalysis we observed by ICP-AES analysis that the molecular catalysts had dissociated from the protein, likely due to catalyst degradation. Thus, an ongoing synthetic challenge is to discover durable molecular catalysts that can withstand constant illumination, stabilize charge accumulation, and support repeated electron- and proton-reduction. An alternative approach is to develop methods to deliver fresh molecular catalyst to PSI to recover photocatalytic activity.

Thylakoid-molecular catalyst hybrids

A key challenge in creating a system that will perform both the reductive and oxidative reactions of photosynthesis is managing disparate kinetics between the two reactions and the mis-match between electron and proton equivalents required for each transformation (here proton reduction and water oxidation). In natural photosynthesis, the thylakoid membrane optimally positions PSI and PSII, manages electron transfer from PSII to PSI with diffusible intermediates, and creates a pH gradient to provide additional reaction driving force. Therefore, we pursued the possibility to create a complete water-splitting system comprised of first-row transition metal molecular catalysts and thylakoid membranes. Overall, molecular catalysts have greater metal atom efficiency than nanoparticle catalysts which typically have many spectator atoms surrounding very few active sites, proposing a pathway for economical and scalable thylakoid-based biohybrids. Similar to the PSI-PtNP biohybrid using isolated PSI,[17] in the thylakoid

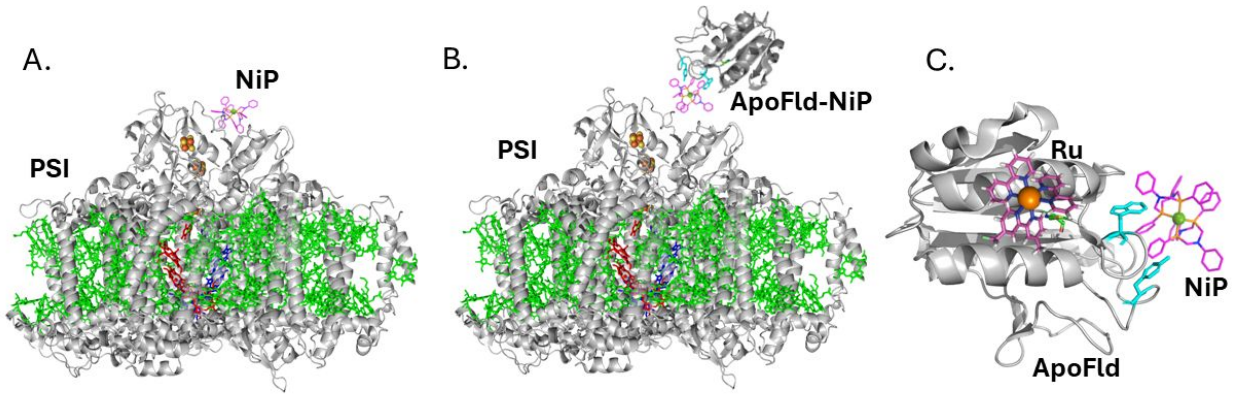

Fig. 7 Different biohybrid constructs for photocatalytic H_2 production from the $[Ni(P_2^{Ph}N_2^{Ph})_2](BF_4)_2$ catalyst (NiP). A. PSI-NiP hybrid uses light-driven charge separation from PSI to drive H_2 production at protein embedded NiP,[34] B. An ApoFld-NiP hybrid delivers the catalyst to the acceptor side of PSI, positioning NiP to receive PSI's light-driven generated electrons,[34] C. Small protein hybrid made photosynthetic via covalent binding of a Ru photosensitizer to Cys54 and NiP insertion into the flavin pocket of ApoFld.[32] (PDB: 1JB0, 1CZL)

membrane PSI's three stromal subunits extend beyond the membrane and were the targeted location for molecular catalyst binding. CoPy and NiP were synthesized according to published methods. [93, 100, 101] Fresh cyanobacterial thylakoids were prepared as described above. To test self-assembly, 200 µM CoPy and NiP were incubated with 0.2 mg ml^{-1} Chl cyanobacterial thylakoid membranes (*S. leopoliensis*) overnight and then pelleted/resuspended multiple times to wash away unassociated catalyst.[56] When 3-(3,4-dichlorophenyl)-1,1-dimethylurea (DCMU) was added to the system to block electron transfer from PSII, sodium ascorbate as SED and cyt c_6 were added to facilitate reduction of $P700^+$, H_2 production for the half-reaction was observed, but at rates 13-fold (for CoPy) and 5-fold (for NiP) lower than rates observed for the comparable thylakoid-PtNP hybrid (Table 1). Despite the lower activity, the observation of H_2 production provided clear evidence that molecular catalysts are functionally positioned at the acceptor end of PSI embedded in the membrane. Z-scheme H_2 and O_2 production were measured for the NiP catalyst by removal of DCMU to open up electron transfer from PSII, and complete water splitting was observed, albeit at low levels. This work provides the first examples of molecular catalysts self-assembling with membrane-bound PSI and proof-of-concept for building completely earth-abundant biohybrid systems that can split water into hydrogen and oxygen. The thylakoid-PtNP and -molecular catalyst biohybrid studies are a step towards *in vivo* approaches to generate living photosynthetic systems as a sustainable energy solution.

Protein-directed delivery of catalysts

A promising method to achieve directed binding of molecular catalysts to PSI involves using an acceptor protein to deliver the catalyst (Fig. 7B). The strategy is two-part: i.) controlled molecular catalyst incorporation into a small protein and ii.) delivery of catalyst in close proximity to the F_B cluster by way of inherent protein-protein electrostatic interactions. The acceptor protein flavodoxin (Fld) was chosen as the catalyst carrying protein to assemble PSI-molecular catalyst hybrids. Fld from *Synechococcus lividus* is a relatively small protein (17 kDa) which contains just one cofactor, a flavin mononucleotide (FMN) that sits within a pocket of the protein secondary structure but is not covalently bonded to any protein residues. We used acid precipitation methods to remove FMN from Fld, and NiP was integrated into the resultant apo-protein during subsequent refolding of the protein (Fig. 6D).[34] We named this hybrid "ApoFld-NiP" (Fig. 7B). Specifically, ApoFld was prepared by treatment of S. lividus Fld with 3 % trichloroacetic acid in the presence of dithiothreitol. The apoprotein was precipitated by centrifugation and the NiP catalyst was added to a final concentration of 40 µM in Hepes buffer, pH 7.3. The ApoFld and NiP solution was incubated in the dark for 2 hours at room temperature. Unbound catalyst was removed from protein-bound complex by microfiltration and ICP-AES was used to determine Ni content for each sample. The ApoFld protein concentration was determined by the Bradford method.[102] NiP incorporation within the FMN binding site was confirmed by competition studies with native FMN cofactor. Photocatalysis experiments with this modified Fld demonstrated a new mechanism for biohybrid creation. The observed rate of photocatalysis for a mixture of PSI and ApoFld-NiP hybrid system nearly doubled and the length of catalysis was extended 30% as compared to catalysis of the directly self-assembled PSI-NiP catalyst hybrid. Therefore, the ApoFld-NiP hybrid delivers the catalyst to the Fld docking site of PSI to facilitate successful placement for efficient photocatalysis. Importantly, the catalyst delivery approach provides self-repair opportunities to introduce fresh catalyst to the acceptor end of PSI, and similar future studies with Fd will impart additional opportunities to create novel protein-delivery solar fuel hybrid systems.

Small Protein Biohybrids

PSI biohybrids are among the best photocatalytic H_2-producing hybrids to date (Table 1). However, PSI's large size and multiple spectroscopically overlapping Fe-S cluster cofactors limit the direct study of catalyst-protein interactions and resolution of electron transfer reactions between PSI and catalyst sites. For this reason, we designed a set of biohybrids that use the small, soluble proteins Fd and Fld as templates for directed binding of both molecular chromophore and catalyst modules (Fig. 7C).[31-33] In this manner, these small electron carrier proteins Fd and Fld were turned into photosynthetic proteins which enable spectroscopic characterization of electron transfer processes related to catalysis.

Two distinct methods were developed for incorporation of cobaloxime catalysts into the protein matrices of Fd and Fld (Fig. 8). The $CoBF_2$ derivative was chosen for the first hybrid studies due to its spectroscopically detectable Co(II) ground state. Active spinach Fd was purchased from Sigma-Aldrich. The Fd-$CoBF_2$ hybrid was synthesized by addition of 4 mol equiv. of $CoBF_2$ to 100 – 500 µM Fd in 20 mM Hepes, pH 7.9. The mixture was incubated for 2 hours in the dark at room temperature. Unbound catalyst was removed from the hybrid complex by the use of 3000 MWCO filtration devices. $CoBF_2$ was covalently bound to a surface histidine residue of Fd via axial ligation to the cobalt center, which was verified by observation of the N hyperfine splitting in the low temperature X-band EPR

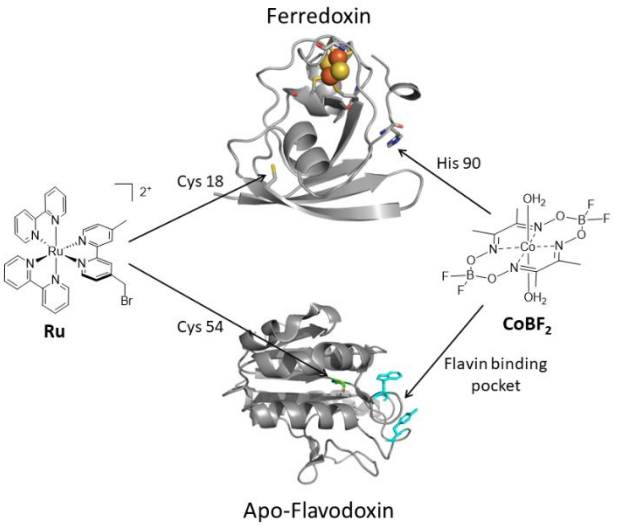

Fig. 8 Construction of small photosynthetic biohybrids. The Ru-Fd-$CoBF_2$ hybrid is made by covalent binding of [Ru(4-CH_2Br-4'-CH_3-2,2'-bpy)(bpy)$_2$]·2PF_6 (Ru) to Cys 18 and Co(dmgBF_2)$_2$·2H_2O ($CoBF_2$) to His90 of Fd (1A70). The Ru-ApoFld-$CoBF_2$ is prepared by covalent binding of Ru to Cys54 of ApoFld-$CoBF_2$ in which $CoBF_2$ is inserted in the flavin binding pocket of Fld (PDB: 1CZL).

spectrum of the Co(II) center.[33] For Fld, which does not contain a histidine for ligation, $CoBF_2$ was inserted in the binding pocket of the

native FMN cofactor by the method determined for the ApoFld-NiP hybrid described above.[31] To add light-harvesting and electron transfer functionalities, the photosensitizer molecule, [Ru(4-CH_2Br-4'-CH_3-2,2'-bpy)(bpy)$_2$]$^{2+}$ (Ru) was bound via bromine substitution to free cysteine residues provided by Fd (Cys18) and Fld (Cys54).[31, 33] 2 mol equiv. of Ru was added to 100 – 250 μM solutions of the Fd-$CoBF_2$ and ApoFld-$CoBF_2$ hybrids and incubated in the dark for 2 hours at room temperature. Repeated concentration/wash steps with 3000 MWCO microfiltration devices were used to remove unbound Ru from the protein hybrid complexes. The resultant Ru-Fd-$CoBF_2$ and Ru-ApoFld-$CoBF_2$ biohybrids were studied with EPR spectroscopy, examining both the coordination environments of Co(II) and light-induced oxidation state changes to the Co(II) and Ru(II) ground states.[31, 33] Transient absorption spectroscopy was used to resolve the formation and decay of Ru and Co related species in the catalytic cycle of each biohybrid. Although similar constructs, the electron transfer pathway in each biohybrid is different; sequential vs. direct depending on the native cofactors (Scheme 1).[31] The charge-separated state of Ru(III)-Fd-Co(I) is formed via an electron relay through the Fd [2Fe-2S] cluster, and is particularly long-lived at ~6 ms, persisting long enough to initiate the catalytic cycle for $2H^+ + 2e^- \rightarrow H_2$. In contrast, direct electron transfer occurs between Ru and Co in the Ru-ApoFld-$CoBF_2$ hybrid, wherein a Ru(I)-ApoFld-Co(I) charge separated state (~2.6 ms) is formed via a reductive quenching mechanism. As with RCs, the intermediary protein environment between electron donor and acceptor molecules stabilizes the charge separated state on the milliseconds timescale, which helps to facilitate catalysis. We determined the quantum efficiencies for the two-electron process of H_2 production to be 1.0 ± 0.3 % for Ru-Fd-$CoBF_2$ and 0.4 ± 0.1 % for Ru-ApoFld-$CoBF_2$. A second Ru-Fd-Co hybrid was prepared with CoPy and performed photocatalysis at rates 3-fold faster than the $CoBF_2$ hybrid.

The ApoFld-NiP hybrid was turned into a photocatalyst by covalent linkage of Ru to the free cysteine residue Cys54.[32] The resultant Ru-ApoFld-NiP hybrid protein environment enables unprecedented performance of NiP over wide pH range, from pH 3.5 to 12. We observed that NiP readily degrades in water and precipitates out of aqueous solution even at micromolar concentrations. However, once NiP is incorporated with Fld, we observe photocatalytic activity from the biohybrid, suggesting that the catalyst is stabilized in the protein pocket. Further, we have observed that the ApoFld-NiP assembly is stable for days on ice, and for months in the freezer (Fig. 6D), evidenced by continued activity for aqueous H_2 production after multiple freeze-thaw cycles. Thus, the protein environment helps stabilize the catalyst in aqueous solution. This concept can be generalized with molecular catalysts since they can be tuned through known synthetic modifications and will enable future modular creation of multiple hybrid systems with different functions.

Interprotein electron transfer biohybrid

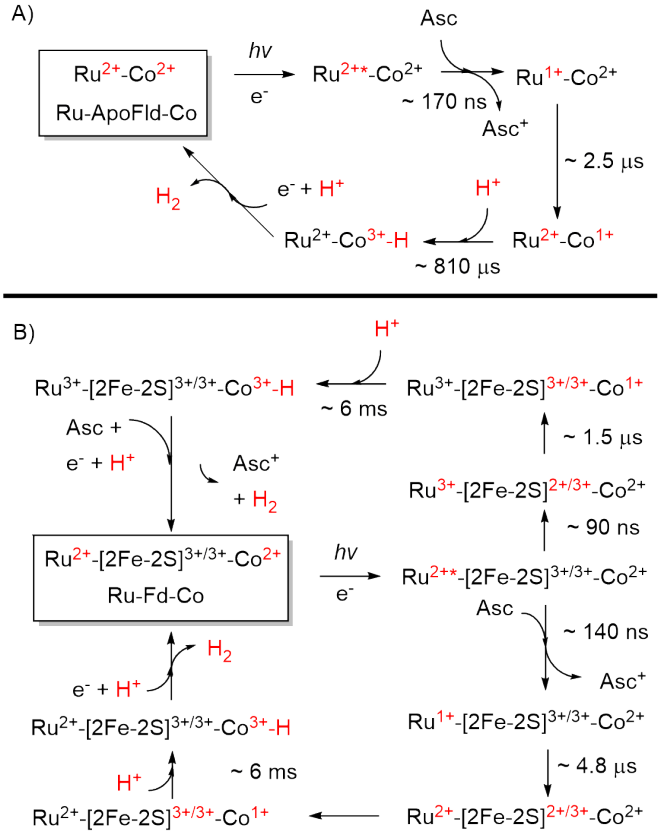

Scheme 1. Proposed catalytic cycles of both Ru-Fd-$CoBF_2$ and Ru-ApoFld-$CoBF_2$ as observed by EPR and transient optical kinetic studies. A) Ru-ApoFld-$CoBF_2$ pathway is unidirectional using a reductive quenching pathway that produces H_2. B. Ru-Fd-$CoBF_2$ pathway is bidirectional with an oxidative quenching pathway (top) as the primary pathway to H_2 production as observed by EPR. There is evidence for a small component of the reductive quenching pathway (bottom), which can continue on to perform H_2 through the above scheme. Reproduced from reference. [31]

Table 1. Comparison of rates of light-induced H_2 production for PSI and thylakoid biohybrid systems.

System	catalyst	SED[a]	TOF [mol H_2 (mol PSI)$^{-1}h^{-1}$]
PSI, long-lived[b]	Pt, photoprecipitated	yes	7.2
PSI, short lived[b]	Pt, photoprecipitated	yes	468
PSI[c]	Ni diphosphine	yes	2,600
PSI, molecular wire, mutated F_B[d]	PtNP	yes	4,200
PSI, protein delivery[c]	NiApoFld	yes	4,500
PSI[e]	cobaloxime	yes	10,200
PSI[f]	PtNP	yes	21,000
Thylakoid, *spinach*[g]	PtNP	yes	>2,100
Thylakoid, *spinach*[g]	PtNP	no	>50
Thylakoid, *S. leopoliensis*[g]	PtNP	yes	1500
Thylakoid, *S. leopoliensis*[g]	PtNP	no	40
Thylakoid, *S. leopoliensis*[g]	Ni diphosphine	yes	320
Thylakoid, *S. leopoliensis*[g]	Ni diphosphine	no	3
Thylakoid, *S. leopoliensis*[g]	cobaloxime	yes	110

[a]Sacrificial electron donor: 100 mM sodium ascorbate. [b]Ref 54. [c]Ref 34. [d]Ref 16.[e]Ref 55. [f]Ref 17. [g]Ref 56.

We expanded on the small protein biohybrid work to utilize protein-protein interactions in a fuel generation scheme. Following light-induced charge separation in PSI, Fd shuttles the light-generated electron it receives from PSI to the Fd-$NADP^+$ reductase (FNR) enzyme for NADPH generation. We reengineered this Fd/FNR subset of the native photosynthetic electron transfer chain for H_2 production by construction of the Ru-Fd hybrid (Fig. 8) and adding catalytic function to its partner protein FNR by attachment of $CoBF_2$ (Fig. 9).[103] FNR was overexpressed from a synthetic gene and purified as previously described.[103] FNR activity was confirmed by NADP+ reduction assays. [82] The FNR-$CoBF_2$ hybrid was prepared by addition of 10 mol equiv. of $CoBF_2$ to a 20-50 µM solution of FNR in 20 mM Hepes pH 8.0. The mixture was incubated overnight at 4 °C followed by repeated concentration/wash steps with Hepes buffer through 10,000 MWCO microfiltration devices to remove unbound catalyst. We confirmed that $CoBF_2$ coordinates directly with Anabaena FNR via Co(II) His and/or Glu/Asp coordination as confirmed by EPR spectroscopy, and appears in a ratio of 1.4 ± 0.3 Co/FNR quantified by ICP-AES analysis. A mixture of the Ru-Fd and FNR-$CoBF_2$ hybrids in solution with a SED readily generates H_2 under blue light illumination. The observed rates of photocatalysis increased with increased ratios of Fd to FNR up to 72 Fd: 1 FNR. Variation of salt concentration showed that the photocatalytic rates also depend on ionic strength with 200 mM NaCl increasing H_2 production compared to no salt, but a further increase in ionic strength to 1 M NaCl hindered H_2 production. These results are consistent with electrostatic interactions known to be important for association of these two proteins.[73] This 2-protein system produces H_2 with TON > 2500 H_2/FNR,[103] which is a significant improvement in TON in comparison to the corresponding single protein Ru-Fd-$CoBF_2$ (210 TON) and Ru-ApoFld-$CoBF_2$ (85 TON) hybrids that rely on *intra*-protein electron transfer between abiotic cofactors.[31] We removed the FeS cluster of Fd and the flavin adenine dinucleotide (FAD) of FNR and showed that neither cofactor is essential for the electron

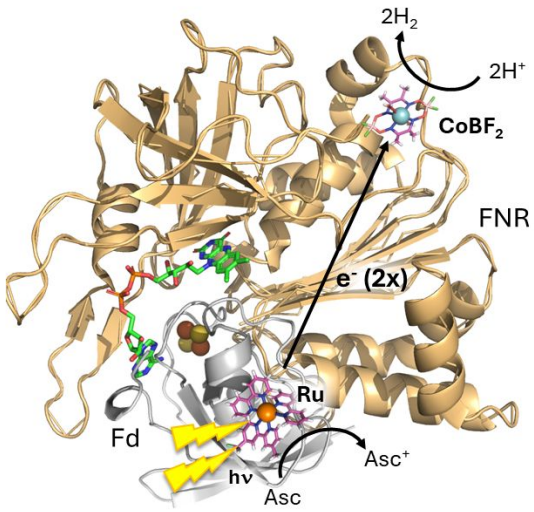

Fig. 9 Proposed scheme of photocatalytic H_2 generation initiated by inter-biohybrid electron transfer, specifically from the photosensitizer on Ru-Fd hybrid to the $CoBF_2$ catalyst on the FNR-$CoBF_2$ hybrid. (PDB: 1A70, 2BSA)

transfer relays between Ru and $CoBF_2$, thus demonstrating that photocatalysis occurs via a direct electron transfer mechanism.[103] This highly active two protein biohybrid system provides an example of how to incorporate catalytic function into larger photosynthetic relays and utilize interprotein electron transfer to achieve catalysis.

Photosynthetic biohybrid charge accumulation

A new direction for biohybrid research is to utilize biohybrids to uniquely interrogate nature's mechanisms for converting light energy to chemical energy. In a first-of-a-kind study, we used Ru-Fd and Ru-Fld hybrids to study photosynthetic coupling of one electron transfers to charge accumulation at the FNR enzyme.[104] FNR contains a single FAD cofactor is known to stabilize three distinct oxidation states: fully oxidized, partially reduced by one electron (semiquinone), and fully reduced by two electrons (hydroquinone). Rather than transfer two single electrons and one proton, FNR instead pairs two single electrons from reduced Fd (or Fld) with one proton transfer into a combined single hydride transfer step to protein bound substrate $NADP^+$.[105] Because the FNR protein stabilizes the hydroquinone state, the reduction potential for the semiquinone/hydroquinone couple is very similar to that for the oxidized/semiquinone couple, rendering it extremely difficult to isolate and spectroscopically detect the intermediate semiquinone in the native system. However, by augmenting the electron transfer function of Fd and Fld with visible light-harvesting ability of Ru, we were able to use the light-driven electron transfer function of the Ru-Fd and Ru-Fld biohybrids to generate the semiquinone of FNR.[104] Freeze quenching the two-protein systems (Ru-Fd + FNR and Ru-Fld + FNR) under illumination readily generated the semiquinone state of FNR as observed with cw EPR spectroscopy. Utilizing a selective deuteration approach that our group pioneered to observe interquinone electron transfer in bacterial RCs,[106-109] we successfully spectroscopically distinguished the flavin cofactors of Fld and FNR with EPR and directly observed inter-flavoprotein electron transfer reaction. We observed a 13% stabilization of the maximal amount of semiquinone, which is the range of 10 – 20% reported for FNR protein stabilization and consistent, in general, with flavoproteins that transfer two electrons at a time.[110, 111]

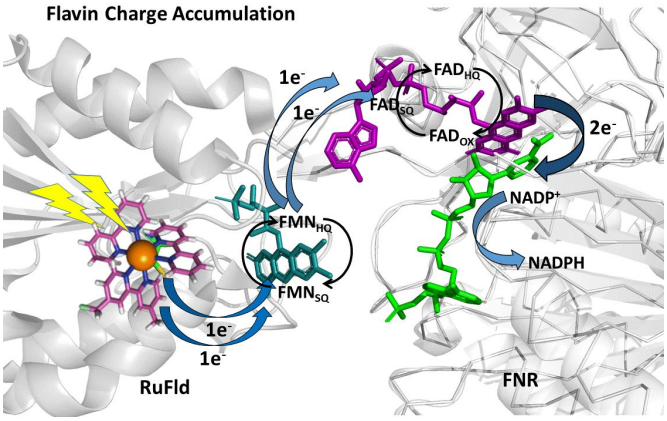

Fig. 10 Scheme of photosynthetic electron transfer between Ru-Fld and FNR highlighting the multielectron capabilities of the flavin cofactors. To initiate the interprotein electron transfer, Fld_{ox} must obtain two electrons from single electron transfers from Ru covalently bound to Cys54 (Ru is rereduced via the sacrificial electron donor sodium ascorbate). The Fld cofactor then cycles between the Fld_{SQ} and Fld_{HQ} transferring electrons one at a time to FNR. FNR_{HQ} then donates 2 electrons and a proton in one step via a hydride to bound $NADP^+$ to form NADPH. Fld_{SQ} and FNR_{SQ} are observable via EPR. Figure reproduced from reference [99].

Interestingly, even though we measured no difference in NADPH production in the native electron transfer pathway from PSI to FNR using either Fd or Fld, we observed a notable distinction in NADPH production between the Ru-Fd and Ru-Fld biohybrid systems.[104] Ru-Fld exhibited an 8-fold higher rate of $NADP^+$ reduction and nearly double the number of turnovers than that reduced by Ru-Fd. A clear and obvious difference between the two systems is the nature of the cofactors of Fd and Fld, a [2Fe2S] cluster and a flavin molecule, respectively. We hypothesize that the versatility of the flavin cofactor of Fld that has three oxidation states readily available and able to collect two electrons, can more easily accommodate a hydride transfer (two electrons and one proton) than the single electron carrier capability of the [2Fe2S] cluster of Fd (Fig. 10). These observations, uniquely revealed by the biohybrid systems, form the benchmark for the relevant spectroscopic response to enable follow-on studies using the semiquinone state as a marker for photosynthetic electron transfer steps, and have revealed an important mechanism for effective photosynthetic coupling of one electron transfers to charge accumulation.

Conclusions and outlook

RC and RC-inspired biohybrid systems highlight the incredible scientific opportunities that exist by combining synthetic catalysts with evolved protein structures for photons-to-fuels research. Our contribution to RC biohybrid research is the development of targeted self-assembling strategies for PSI-catalyst hybrid formation that enable efficient coupling of PSI's highly evolved light capture and conversion capabilities to abiotic catalysts inserted into the protein matrix. We demonstrated that these self-assembling strategies developed for isolated PSI also translate to PSI when it is embedded in its native thylakoid membrane environment, and subsequently created thylakoid hybrids capable of complete solar water splitting. The extensive variety of known transition metal coordination complexes provide numerous possibilities for future innovative RC-catalyst designs. Protein-directed delivery utilizes inherent protein-protein interactions for molecular catalyst hybrid incorporation and provides a unique strategy to explore for self-repair of PSI and thylakoid biohybrid systems. These studies are a step toward redirecting PSI reduction equivalents to drive catalytic reactions from abiotic molecular catalysts *in vivo*, overcoming the inherent inefficiencies of photosynthesis to generate living photosynthetic systems as a sustainable energy solution. Broad research challenges remain, include developing methods to enable entry of molecular catalysts into living systems and synthetically tune the molecules and biogenetically engineer PSI to target catalyst-protein interactions *in vivo*.

Additionally, we have innovated RC-inspired biohybrid designs that use small proteins as scaffolds for the directed binding of both light harvesting and catalyst molecules. The resultant small photosynthetic biohybrid designs both facilitate H_2 evolution activity at near neutral pH by stabilization of charge separation and enable spectroscopic delineation of light-driven electron transfer processes related to proton reduction. These systems provide a benchmark for future development of biohybrids to support and protect important catalytic systems in aqueous environments through protein engineering and design. A new direction of biohybrid research is to incorporate synthetic molecules to creatively probe

nature's mechanisms, such as flavin electron transfer chains in biology. Our hope is that light-driven capabilities of biohybrid systems will be used to delineate mechanisms of complex multi-redox enzymatic reactions in biology.

Another future direction for RC biohybrid research is to build on the knowledge gained from photocatalytic H_2 evolution to develop and study biohybrid mechanisms for CO_2 photoreduction. The coupling of nature's optimized RC photochemistry to light-driven transformation of CO_2 to fuels such as methane or methanol, a liquid fuel, would be a big achievement. Importantly, this work could provide a way to decrease environmentally harmful CO_2, the most abundant greenhouse gas. To achieve this challenge, a multidisciplinary research effort from biologists and chemists is needed to engineer durable, earth abundant biohybrid systems that can withstand multiple turnovers in aqueous solutions and make sunlight a cost-effective, storable and transportable resource for large scale utilization.

Author Contributions

LMU and KLM wrote the manuscript and prepared the figures.

Conflicts of interest

There are no conflicts to declare.

Acknowledgements

This work is supported by the U. S. Department of Energy, Office of Science, Office of Basic Energy Sciences, Division of Chemical Sciences, Geosciences, Biosciences, under Contract No. DE-AC02-06CH11357.

Notes and references

1. R. E. Blankenship, *Molecular Mechanisms of Photosynthesis*, Blackwell Science Ltd, Malden, USA, 2002.
2. D. Gust, T. A. Moore and A. L. Moore, *Acc. Chem. Res.*, 2009, **42**, 1890-1898.
3. L. Hammarstrom, *Curr. Opin. Chem. Biol.*, 2003, **7**, 666-673.
4. M. R. Wasielewski, *Acc. Chem. Res.*, 2009, **42**, 1910-1921.
5. L. Hammarstrom, *Acc. Chem. Res.*, 2015, **48**, 840-850.
6. A. J. Morris, G. J. Meyer and E. Fujita, *Acc. Chem. Res.*, 2009, **42**, 1983-1993.
7. P. W. Du, J. Schneider, G. G. Luo, W. W. Brennessel and R. Eisenberg, *Inorg. Chem.*, 2009, **48**, 4952-4962.
8. A. Fihri, V. Artero, M. Razavet, C. Baffert, W. Leibl and M. Fontecave, *Angew. Chem. Int. Ed.*, 2008, **47**, 564-567.
9. F. Lakadamyali and E. Reisner, *Chem. Commun.*, 2011, **47**, 1695-1697.
10. K. L. Mulfort and L. M. Utschig, *Acc. Chem. Res.*, 2016, **49**, 835-843.
11. R. E. Blankenship, D. M. Tiede, J. Barber, G. W. Brudvig, G. Fleming, M. Ghirardi, M. R. Gunner, W. Junge, D. M. Kramer, A. Melis, T. A. Moore, C. C. Moser, D. G. Nocera, A. J. Nozik, D. R. Ort, W. W. Parson, R. C. Prince and R. T. Sayre, *Science* 2011, **332**, 805-809.
12. A. Melis, *Plant Sci.*, 2009, **177**, 272-280.
13. E. Greenbaum, *Science*, 1985, **230**, 1373-1375.
14. L. M. Utschig, S. R. Soltau and D. M. Tiede, *Curr. Opin. Chem. Biol.*, 2015, **25**, 1-8.
15. B. R. Evans, H. M. O'Neill, S. A. Hutchens, B. D. Bruce and E. Greenbaum, *Nano Lett.*, 2004, **4**, 1815-1819.
16. R. A. Grimme, C. E. Lubner, D. A. Bryant and J. H. Golbeck, *J. Am. Chem. Soc.*, 2008, **130**, 6308-6309.
17. L. M. Utschig, N. M. Dimitrijevic, O. G. Poluektov, S. D. Chemerisov, K. L. Mulfort and D. M. Tiede, *J. Phys. Chem. Lett.*, 2011, **2**, 236-241.
18. P. W. King, *Biochim. Biophys. Acta Bioenerg.*, 2013, **1827**, 949-957.
19. C. E. Lubner, A. M. Applegate, P. Knorzer, A. Ganago, D. A. Bryant, T. Happe and J. H. Golbeck, *Proc. Natl. Acad. Sci. U.S.A.*, 2011, **108**, 20988-20991.
20. M. Bacchi, G. Berggren, J. Niklas, E. Veinberg, M. W. Mara, M. L. Shelby, O. G. Poluektov, L. X. Chen, D. M. Tiede, C. Cavazza, M. J. Field, M. Fontecave and V. Artero, *Inorg. Chem.*, 2014, **53**, 8071-8082.
21. A. Onoda, Y. Kihara, K. Fukumoto, Y. Sano and T. Hayashi, *ACS Catal.*, 2014, **4**, 2645-2648.
22. J. W. Slater and H. S. Shafaat, *J. Phys. Chem. Lett.*, 2015, **6**, 3731-3736.
23. D. J. Sommer, M. D. Vaughn and G. Ghirlanda, *Chem. Commun.*, 2014, **50**, 15852-15855.
24. D. J. Sommer, M. D. Vaughn and G. Ghirlanda, *Biochim. Biophys. Acta Bioenerg.*, 2016, **1857**, 598-603.
25. A. Call, C. Casadevall, A. Romero-Rivera, V. Martin-Diaconescu, D. J. Sommer, S. Osuna, G. Ghirlanda and J. Lloret-Fillol, *ACS Catal.*, 2019, **9**, 5837-5846.
26. E. H. Edwards, J. Jelusic, S. Chakraborty and K. L. Bren, *J. Inorg. Biochem.*, 2021, **217**, 111384.
27. S. M. Parambath, D. Prakash, W. Swetman, A. Surakanti and S. Chakraborty, *Chem. Commun.*, 2023, **59**, 13325.
28. C. R. Schneider and H. S. Shafaat, *Chem. Commun.*, 2016, **52**, 9889-9892.
29. S. C. Marguet, M. J. Stevenson and H. S. Shafaat, *J. Phys. Chem. B*, 2019, **8**, 9792-9800.
30. L. Shi, T. C. Squier, J. M. Zachara and J. K. Fredrickson, *Molec. Microbiol.*, 2007, **65**, 12-20.
31. S. R. Soltau, P. D. Dahlberg, J. Niklas, O. Poluektov, K. L. Mulfort and L. M. Utschig, *Chem. Sci.*, 2016, **7**, 7068-7078.
32. S. R. Soltau, J. Niklas, P. D. Dahlberg, K. L. Mulfort, O. G. Poluektov and L. M. Utschig, *ACS Energy Lett.*, 2017, **2**, 230-237.
33. S. R. Soltau, J. Niklas, P. D. Dahlberg, O. G. Poluektov, D. M. Tiede, K. L. Mulfort and L. M. Utschig, *Chem. Commun.*, 2015, **51**, 10628-10631.
34. S. C. Silver, J. Niklas, P. Du, O. G. Poluektov, D. M. Tiede and L. M. Utschig, *J. Am. Chem. Soc.*, 2013, **135**, 13246-13249.
35. K. A. Brown and P. W. King, *Photosyn. Res.*, 2020, **143**, 193-203.
36. A. W. Harris and J. N. Cha, *Mol. Syst. Des. Eng.*, 2020, **5**, 1088-1097.
37. K. A. Brown, S. Dayal, X. Ai, G. Rumbles and P. W. King, *J. Am. Chem. Soc.*, 2010, **132**, 9672-9680.
38. K. A. Brown, D. F. Harris, M. B. Wilker, A. Rasmussen, N. Khadka, H. Hamby, S. Keable, G. Dukovic, J. W. Peters, L. C. Seefeldt and P. W. King, *Science*, 2016, **352**.
39. K. A. Brown, M. B. Wilker, M. Boehm and G. Dukovic, *J. Am. Chem. Soc.*, 2012, **134**, 5627-5636.

40. C. A. Caputo, L. Wang, R. Beranek and E. Reisner, *Chem. Sci.*, 2015, **6**, 5690-5694.
41. G. A. M. Hutton, B. Reuillard, C. M. Martindale, C. A. Caputo, C. W. J. Lockwood, J. N. Butt and E. Reisner, *J. Am. Chem. Soc.*, 2016, **138**, 16722-16730.
42. M. Miller, W. E. Robinson, A. R. Oliveira, N. Heidary, N. Kornienko, J. Warnan, I. A. C. Pereira and E. Reisner, *Angew. Chem.*, 2019, **131**, 4649-4653.
43. T. W. Woolerton, S. Sheard, E. Reisner, E. Pierce, S. W. Ragsdale and F. A. Armstrong, *J. Am. Chem. Soc.*, 2010, **132**, 2132-2133.
44. D. K. Dogutan and D. G. Nocera, *Acc. Chem. Res.*, 2019, **52**, 3143-3148.
45. N. Kornienko, J. Z. Zhang, K. K. Sakimoto, P. Yang and E. Reisner, *Nat. Nanotechnol.*, 2018, **13**, 890-899.
46. P. Yang, *Nano Lett.*, 2021, **21**, 5453-5456.
47. J. G. Kleingardner, B. Kandemir and K. L. Bren, *J. Am. Chem. Soc.*, 2014, **136**, 4-7.
48. A. Roy, C. Madden and G. Ghirlanda, *Chem Commun.*, 2012, **48**, 9816-9818.
49. Y. Sano, A. Onoda and T. Hayashi, *Chem. Commun.*, 2011, **47**, 8229-8231.
50. Y. Sano, A. Onoda and T. Hayashi, *J. Inorg. Biochem.*, 2012, **108**, 159-162.
51. C. R. Schneider, A. C. Manesis, M. J. Stevenson and H. S. Shafaat, *Chem. Commun.*, 2018, **54**, 4681-4684
52. M. Gorka and J. H. Golbeck, *Photosyn. Res.*, 2020, **143**, 155-163.
53. M. Gorka, J. Schartner, A. van der Est, M. Rogner and J. H. Golbeck, *Biochemistry*, 2014, **53**, 2295-2306.
54. I. Iwuchukwu, M. D. Vaughn, N. Myers, H. O'Neill, P. Frymier and B. D. Bruce, *Nat. Nanotechnol.*, 2010, **5**, 73-79.
55. L. M. Utschig, S. C. Silver, K. L. Mulfort and D. M. Tiede, *J. Am. Chem. Soc.*, 2011, **133**, 16334-16337.
56. L. M. Utschig, S. R. Soltau, K. L. Mulfort, J. Niklas and O. Poluektov, *Chem. Sci.*, 2018, **9**, 8504-8512.
57. O. G. Poluektov, J. Niklas and L. M. Utschig, *J. Phys. Chem. B*, 2019, **123**, 7536-7544.
58. O. G. Poluektov, S. V. Paschenko, L. M. Utschig, K. V. Lakshmi and M. C. Thurnauer, *J. Am. Chem. Soc.*, 2005, **127**, 11910-11911.
59. O. G. Poluektov and L. M. Utschig, *J. Phys. Chem. B*, 2015, **119**, 13771-13776.
60. O. G. Poluektov, L. M. Utschig, S. L. Schlesselman, K. V. Lakshmi, G. W. Brudvig, G. Kothe and M. C. Thurnauer, *J. Phys. Chem. B*, 2002, **106**, 8911-8916.
61. J. K. Bindra, J. Niklas, Y. Jeong, A. W. Jasper, M. Kretzschmar, J. Kern, L. M. Utschig and O. G. Poluektov, *J. Phys. Chem. B*, 2023, **127**, 10108-10117.
62. P. Jordan, P. Fromme, H. T. Witt, O. Klukas, W. Saenger and N. Krauss, *Nature*, 2001, **411**, 909-917.
63. C. E. Lubner, R. A. Grimme, D. A. Bryant and J. H. Golbeck, *Biochemistry,* 2010, **49**, 404-414.
64. A. Kanygin, Y. Milrad, C. Thummala, K. Reifaschneider, P. Baker, P. Marco, I. Yacoby and K. E. Redding, *Energy Environ. Sci.*, 2020, **13**, 2903-2914.
65. I. Yacoby, S. Pochekailov, H. Toporik, M. L. Ghirardi, P. W. King and S. G. Zhang, *Proc. Natl. Acad. Sci. U.S.A.*, 2011, **108**, 20988-20991.
66. M. Gorka, A. Perez, C. S. Baker, B. Ferlez, A. van der Est, D. A. Bryant and J. H. Golbeck, *J. Photochem. Photobio. B*, 2015, **152**, 325-334.
67. R. A. Grimme, C. E. Lubner and J. H. Golbeck, *Dalton Trans.*, 2009, **45**, 10106-10113.
68. J. F. Millsaps, B. D. Bruce, J. W. Lee and E. Greenbaum, *Photochem. Photobiol.*, 2001, **73**, 630-635.
69. E. Greenbaum, *J. Phys. Chem.*, 1988, **92**, 4571-4574.
70. J. W. Lee, I. Lee and E. Greenbaum, *J. Phys. Chem. Lett.*, 2005, **109**, 5409-5413.
71. J. W. Lee, C. V. Tevault, S. L. Balankinship, R. T. Collins and E. Greenbaum, *Energy & Fuels*, 1994, **8**, 770-773.
72. I. Caspy, A. Borovikova-Sheinker, D. Klaiman, Y. Shkolnisky and N. Nelson, *Nat. Plants*, 2020, **6**, 1300-1305.
73. M. Medina, *FEBS J.*, 2009, **276**, 3942-3958.
74. S. Chen and K. Kimura, *J. Phys. Chem. B*, 2001, **105**, 5397.
75. M. Rogner, P. J. Nixon and B. A. Diner, *J. Biol. Chem.*, 1990, **265**, 6189-6196.
76. L. M. Utschig, L. X. Chen and O. G. Poluektov, *Biochemistry*, 2008, **47**, 3671-3676.
77. L. M. Utschig, D. M. Tiede and O. G. Poluektov, *Biochemistry*, 2010, **49**, 9682-9684.
78. L. M. Utschig, N. J. Zaluzec, T. Malavath, N. S. Ponomarenko and D. M. Tiede, *Biochim. Biophys. Acta Bioenerg.*, 2023, **1864**, 148974.
79. P. Cao, D. Cao, L. Si, X. Su, L. Tian, W. Chang, Z. Liu, X. X. Zhang and M. Li, *Nat. Plants*, 2020, **6**, 167-176.
80. C. J. Gisriel, D. A. Flesher, G. Shen, J. Wang, M. H. Ho, G. W. Brudvig and D. A. Bryant, *J. Biol. Chem.*, 2021, **298**, 101408.
81. H. Kubota-Kawai, R. Mutoh, K. Shinmura, P. Setif, M. M. Nowaczyk, M. Rogner, T. Ikegami, H. Tanaka and G. Kurisu, *Nat. Plants*, 2018, **4**, 218-224.
82. L. M. Utschig, C. L. Duckworth, J. Niklas and O. G. Poluektov, *Photosyn. Res.*, 2024, DOI: 10.1007/s11120-023-01072-4.
83. J. D. Blakemore, R. H. Crabtree and G. W. Brudvig, *Chem. Rev.*, 2015, **115**, 12974-13005.
84. D. Dolui, S. Ghorai and A. Dutta, *Coord. Chem. Rev.*, 2020, **416**, 213335.
85. M. R. Dubois and D. L. Dubois, *Acc. Chem. Res.*, 2009, **42**, 1974-1982.
86. R. W. Hogue, O. Schott, G. S. Hanan and S. Brooker, *Chem. Eur. J.*, 2018, **24**, 9820-9832.
87. J. W. Jurss, R. S. Khnayzer, J. A. Panetier, K. A. El Roz, E. M. Nichols, M. Head-Gordon, J. R. Long, F. N. Castellano and C. J. Chang, *Chem. Sci.*, 2015, **6**, 4954-4972.
88. N. Queyriaux, R. T. Jane, J. Massin, V. Artero and M. Chavarot-Kerlidou, *Coord. Chem. Rev.*, 2015, **304-305**, 3-19.
89. A. Bakac, M. E. Brynildson and J. H. Espenson, *Inorg. Chem.*, 1986, **25**, 4108-4114.
90. X. L. Hu, B. S. Brunschwig and J. C. Peters, *J. Am. Chem. Soc.*, 2007, **129**, 8988-8998.
91. P. A. Jacques, V. Artero, J. Pecaut and M. Fontecave, *Proc. Natl. Acad. Sci. U.S.A.*, *106*, 2009, 20627-20632.
92. M. Razavet, V. Artero and M. Fontecave, *Inorg. Chem.*, 2005, **44**, 4786-4795.
93. W. C. Trogler, R. C. Stewart, L. A. Epps and L. G. Marzilli, *Inorg. Chem.*, 1974, **13**, 1564-1570.
94. G. W. Wangila and R. B. Jordan, *Inorg. Chim. Acta*, 2005, **358**, 2804-2812.
95. M. L. Helm, M. P. Stewart, R. M. Bullock, M. R. DuBois and D. L. DuBois, *Science*, 2011, **333**, 863-866.
96. M. Rakowski DuBois and D. L. DuBois, *Acc. Chem. Res.*, 2009, **42**, 1974-1982.

97. A. D. Wilson, R. H. Newell, M. J. McNevin, J. T. Muckerman, M. R. DuBois and D. L. DuBois, *J. Am. Chem. Soc.*, 2006, **128**, 358-366.
98. M. P. McLaughlin, T. M. McCormick, R. Eisenberg and P. L. Holland, *Chem. Commun.*, 2011, **47**, 7989-7991.
99. A. D. Wilson, R. K. Shoemaker, A. Miedaner, J. T. Muckerman, D. L. DuBois and M. R. DuBois, *Proc. Natl. Acad. Sci. U.S.A.*, 2007, **104**, 6951-6956.
100. G. Markl, G. Y. Jin and C. Schoerner, *Tetrahedron Lett.*, 1980, **21**, 1409-1412.
101. A. D. Wilson, R. H. Newell, M. J. McNevin, J. T. Muckerman, M. R. DuBois and D. L. DuBois, *J. Am. Chem. Soc.*, 2006, **128**, 358-366.
102. M. M. Bradford, *Anal. Biochem.*, 1976, **72**, 248-254.
103. U. Brahmachari, P. R. Pokkuluri, D. M. Tiede, J. Niklas, O. G. Poluektov, K. L. Mulfort and L. M. Utschig, *Photosyn. Res.*, 2020, **143**, 183-192.
104. L. M. Utschig, U. Brahmachari, K. L. Mulfort, J. Niklas and O. G. Poluektov, *Chem. Sci.*, 2022, **13**, 6502-6511.
105. J. K. Hurley, G. Tollin, M. Medina and C. Gomez-Morena, in *Photosystem I: the light-driven plastocyanin:ferredoxin oxidoreductase*, Springer, Dordrecht, 2006, pp. 455-476.
106. O. G. Poluektov and L. M. Utschig, *J. Phys. Chem. B*, 2021, **125**, 4025-4030.
107. O. G. Poluektov, L. M. Utschig, A. A. Dubinskij and M. C. Thurnauer, *J. Am. Chem. Soc.*, 2004, **126**, 1644-1645.
108. O. G. Poluektov, L. M. Utschig, A. A. Dubinskij and M. C. Thurnauer, *J. Am. Chem. Soc.*, 2005, **127**, 4049-4059.
109. L. M. Utschig, M. C. Thurnauner, D. M. Tiede and O. G. Poluektov, *Biochemistry,* 2005, **44**, 14131-14142.
110. M. E. Corrando, A. Aliverti, G. Zanetti and S. G. Mayhew, *Eur. J. Biochem.*, 1996, **239**, 662-667.
111. P. Mulo and M. Medina, *Photosyn. Res.*, 2017, **134**, 265-280.

Data Statement

No primary research results, software or code have been included and no new data were generated or analyzed as part of this review.